Journal of Molecular Structure 1199 (2020) 127059

Contents lists available at ScienceDirect

Journal of Molecular Structure

journal homepage: http://www.elsevier.com/locate/molstruc

Bidentate ligands and their Cu(II) complexes: Structural characterization, electrochemical properties and biological evaluation

Ferhan Tümer [a], Seyit Ali Güngör [a], Muhammet Köse [a], Feridun Koçer [b], Mehmet Tümer [a, *]

[a] Chemistry Department, K.Maras Sütcü Imam University, 46100, K.Maras, Turkey
[b] Bioengineering Sciences, K.Maras Sütcü Imam University, 46100, K.Maras, Turkey

ARTICLE INFO

Article history:
Received 25 June 2019
Received in revised form
9 September 2019
Accepted 10 September 2019
Available online 11 September 2019

Keywords:
Schiff base
X-ray
Electrochemistry
Thermal
Bidentate
Biological activity

ABSTRACT

In this manuscript, three bidentate ligands 2-[(2-methoxybenzylidene)amino]phenol (HA^1), 2-[(3,4,5-trimethoxybenzylidene) amino]phenol (HA^2) and 2-[(2,3,4-trimethoxybenzylidene) amino]phenol (HA^3) were synthesized from the reaction of the 2-aminophenol and methoxy benzaldehyde derivatives in MeOH solution. The Cu^{2+} metal complexes of these ligands were obtained in the 1:1 (M:L) ratio. All the compounds were characterized by the micro analytical and spectroscopic techniques. The single crystals of the bidentate ligands (HA^2 and HA^3) were obtained from the recrystallization from the MeOH solution and their structural characterizations were conducted by the X-ray diffraction method. Antimicrobial activity studies of the bidentate ligands and their Cu^{2+} metal complexes were tested towards *S. aureus, E. coli, B. cereus, B. subtilis, S. typhimurium* as bacteria and *C. albicans* as fungi and the complex Cu^{2+} of the ligand HA^2 showed the highest activity against to the *S. aureus*. While the ligands HA^2 and HA^3 do not show the activity against the bacteria and fungi, the ligand HA^1 has the activity against to the *S. typhimurium, S. aureus* and *C. albicans*. Electrochemical behaviours of all compounds have been investigated in DMF solution and it was found that the cathodic and anodic values of the $[CuA^3(Cl)H_2O]$ complex shifted to the more positive regions owing to the positions of the methoxy groups on the benzaldehyde ring.

1. Introduction

Due to their ease of synthesis and high yields, organic compounds called Schiff bases have been widely used as ligands [1,2]. When Schiff base ligands (also known as imines) have additional donor atoms such as O and N, and they can form a chelate ring forming stable metal complexes. The versatile properties of these compounds have led them to be used in several research areas including the medicine [3], pharmaceutical [4], electronics [5], dyestuffs [6], catalysis [7] and interesting antimicrobial activity [8] studies. Schiff bases, an important class of organic compounds, attract a lot of attention since they are used as models for many biological systems. Biological activity of these compounds is not only dependent on the molecular structure of the compounds. Transition metal complexes of imin ligands sare also very specific because the applications of the organic imine ligands have advanced in coordination with metal ions. The transition metal complexes of the imine ligands are usually shown more biological activity than the corresponding Schiff bases [9].

In the previous studies, the ligands 2-[(2,3,4-trimethoxybenzylidene)amino]phenol and 2-[(3,4,5-trimethoxybenzylidene) amino]phenol were synthesized and characterized by the instrumental methods [10,11]. The cyclometallated complexes were obtained from the reaction of the aromatic imine ligand and $Pd(CH_3COO)_2$ in the toluene solution. The mononuclear $[Pd\{2,3,4\text{-}(MeO)_3C_6HC(H)=N[2\text{-}(O)C_6H_4]\}(PPh_3)]$ complex has been obtained from the reaction of the cyclometallated Pd-complex with $P(PH_3)_3$. On the other hand, the compound (2) was synthesized as a resveratrol derivative and its biological properties was investigated. In this study, all synthesized molecules, resveratrol and its analogues, offered a distinct photoprotection for a single UV-filter substance. E. Tauer and co-workers have reported the photochemical and thermal properties of the aromatic imine ligands obtained from *o*-aminophenol and the carbonyl compounds (aldehydes and/or ketones) [12].

* Corresponding author.
E-mail address: mtumer@ksu.edu.tr (M. Tümer).

https://doi.org/10.1016/j.molstruc.2019.127059
0022-2860/

In this study, we obtained three Schiff bases (HA^1-HA^3) from the *o*-aminophenol and aldehydes (2-methoxy benzaldehyde, 2,3,4-trimethoxy benzaldehyde and 3,4,5- trimethoxy benzaldehyde) and characterized by the spectroscopic and analytical techniques. The Cu^{2+} metal complexes of the ligands were synthesized. The single crystals of the ligands HA^2 and HA^3 were obtained from MeOH solution by the slow evaporation at room temperature and their molecular structures have been examined by the X-ray diffraction method. The electrochemical, thermal and antimicrobial properties of all compounds have been investigated.

2. Methods and materials

2.1. General

All reagents and solvents were of reagent-grade quality and obtained from commercial suppliers (Aldrich or Merck) and used as received, unless otherwise noted. Elemental analyses (C, H, N) were performed using a Costech ECS 4010 (CHN). Infrared spectra were obtained using KBr disc (4000-400 cm^{-1}) on a PerkinElmer Spectrum 100 FT-IR. The electronic spectra in the 200–900 nm range were obtained on a PerkinElmer Lambda 45 spectrophotometer. ^1H and ^{13}C NMR spectra were recorded on a Bruker 400 MHz instrument and TMS was used as an internal standard TMS. Mass spectra of the ligands and their Cu^{2+} metal complexes have recorded on a LC/MS APCI AGILENT 1100 MSD spectrophotometer. Cyclic voltammograms were recorded on a Iviumstat Electrochemical workstation equipped with a low current module (BAS PA–1) recorder.

2.2. Preparation of the 2-aminophenol based Schiff base ligands (HA^1-HA^3)

2-Aminophenol (1 mmol, 0.109 g) was dissolved gently in MeOH (25 mL) and then the solution of the aromatic carbonyl compounds (1 mmol, 0.136 g for 2-methoxybenzaldehyde; 1 mmol, 0.196 g for 2,3,4-trimethoxybenzaldehyde or 3,4,5-trimethoxybenzaldehyde) in MeOH (15 mL) were added to the aminophenol solution with stirring. The solution was refluxed for 2 h at 65 °C. The reaction solution was then allowed to cool to the room temperature. The precipitates were filtered and recrystallized from MeOH and dried in a desiccator.

HA^1: $C_{14}H_{13}NO_2$. Yield: 90%, color: Dark red, melting point: 102–105 °C. Elemental analysis; found (calcd.) %; C, 74.05 (73.99); H, 5.82 (5.77); N, 6.21 (6.16). ^{1}HNMR (δ, $CDCl_3$) 8.58 (s, 1H, CH=N), 7.72–6.28 (m, 8H, aromatic rings-H), 3.90 (s, 3H, *ortho*-OCH_3). ^{13}CNMR (δ, $CDCl_3$) 164.55 (CH=N), 152.20–108.40 (aromatic rings C-atoms), 56.45 (*ortho*-OCH_3-C atom). Mass spectrum (ESI/MS, *m*/*z*): Calcd.: 227.25, found: 228 $[M]^+$; calcd.: 110.13, found: 110 $[C_6H_8NO]^+$. FTIR (KBr, ν, cm^{-1}): 3375 ν(O–H), 2937 $\nu(C-H)_{aliph}$, 1616 ν(C=N), 1486 $\nu(C=C)_{aromatic}$, 1290 $\nu(C-O)_{phenolic}$. UV–vis (DMF, λ_{max}, 1.0×10^{-3} M): 389, 366, 352, 265, 230.

HA^2: $C_{16}H_{17}NO_4$. Yield: 81%, color: Dark red, melting point: 112–115 °C. Elemental analysis; found (calcd.) %; C, 66.93 (66.89); H, 5.98 (5.96); N, 4.93 (4.88). ^{1}H NMR (δ, $CDCl_3$), 8.66 (s, 1H, CH=N), 8.02–6.37 (m, 6H, aromatic rings-H), 3.75 (s, 3H, *meta*-OCH_3), 3.82 (s, 3H, *para*-OCH_3), 3.75 (s, 3H, *meta'*-OCH_3). ^{13}CNMR (δ, $CDCl_3$) 167.80 (CH=N), 158.40–109.15 (aromatic rings C-atoms), 57.55 (*meta*-OCH_3-C atom), 58.10 (*para*-OCH_3-C atom), 57.55 (*meta'*-OCH_3-C atom). Mass spectrum (ESI/MS, *m*/*z*): Calcd.: 287.31, found: 288 $[M]^+$; calcd.: 101.10, found: 101 $[C_7H_3N]^+$. FTIR (KBr, ν, cm^{-1}): 3350 ν(O–H), 2940 $\nu(C-H)_{aliph}$, 1624 ν(C=N), 1485 $\nu(C=C)_{aromatic}$, 1286 $\nu(C-O)_{phenolic}$. UV–vis (DMF, λ_{max}, 1.0×10^{-3} M): 380, 358, 343, 290, 230.

HA^3: $C_{16}H_{17}NO_4$. Yield: 84%, color: Dark red, melting point: 82–85 °C. Elemental analysis; found (calcd.) %; C, 66.94 (66.89); H, 6.11 (5.96); N, 4.94 (4.88). ^{1}H NMR (δ, $CDCl_3$), 8.63 (s, 1H, CH=N), 7.93–6.66 (m, 6H, aromatic rings-H), 3.98 (s, 3H, *ortho*-OCH_3), 3.85 (s, 3H, *meta*-OCH_3), 3.94 (s, 3H, *para*-OCH_3). ^{13}CNMR (δ, $CDCl_3$) 166.15 (CH=N), 159.72–110.44 (aromatic rings C-atoms), 61.50 (*ortho*-OCH_3-C atom), 59.10 (*meta*-OCH_3-C atom), 57.15 (*para*-OCH_3-C atom). Mass spectrum (ESI/MS, *m*/*z*): Calcd.: 287.31, found: 288 $[M]^+$; calcd.: 101.10, found: 101 $[C_7H_3N]^+$. FTIR (KBr, ν, cm^{-1}): 3376 ν(O–H), 2936 $\nu(C-H)_{aliph}$, 1620 ν(C=N), 1485 $\nu(C=C)_{aromatic}$, 1286 $\nu(C-O)_{phenolic}$. UV–vis (DMF, λ_{max}, 1.0×10^{-3} M): 386, 366, 350, 290, 239.

2.3. Preparation of the Cu^{2+} complexes of the bidentate ligands HA^1-HA^3

The ligands HA^1-HA^3 (1 mmol, 0.227 g for HA^1; 1 mmol, 0.288 g for HA^2 and HA^3) have dissolved in MeOH (20 mL). The $CuCl_2 \cdot 2H_2O$ (1 mmol, 0.171 g) dissolved in the MeOH (20 mL) was added to the ligand solution and resulting solution was refluxed for 5–6 h. The reaction solution was cooled to the room temperature and the dark colored precipitates were filtered off, washed with the cold MeOH and finally dried in a desiccator.

$[CuA^1(Cl)(H_2O)]$: $C_{15}H_{16}ClCuNO_4$. Yield: 75%, color: Dark green, melting point: >250 °C. Elemental analysis; found (calcd.) %; C, 49.02 (48.99); H, 4.15 (4.11); N, 4.12 (4.08). Mass spectrum (ESI/MS, *m*/*z*): Calcd.: 373.29, found: 373 $[M]^+$; calcd.: 355.27, found: 356.15 $[M - H_2O]^+$. FTIR (KBr, ν, cm^{-1}): 3342 $\nu(O-H)_{H2O}$, 2948 $\nu(C-H)_{aliph}$, 1596 ν(C=N), 1475 $\nu(C=C)_{aromatic}$, 1243 $\nu(C-O)_{phenolic}$, 542 ν(Cu–O), 478 ν(Cu–N). UV–vis (DMF, λ_{max}, 1.0×10^{-3} M): 505, 440, 334, 291, 276.

$[CuA^2(Cl)(H_2O)]$: $C_{16}H_{18}ClCuNO_5$. Yield: 73%, color: Dark green, melting point: >250 °C. Elemental analysis; found (calcd.) %; C, 47.72 (47.65); H, 4.56 (4.50); N, 3.53 (3.47). Mass spectrum (ESI/MS, *m*/*z*): Calcd.: 403.31, found: 404 $[M]^+$; calcd.: 349.84, found: 350 $[M-H_2O-Cl]^+$. FTIR (KBr, ν, cm^{-1}): 3321 $\nu(O-H)_{H2O}$, 2935 $\nu(C-H)_{aliph}$, 1600 ν(C=N), 1500 $\nu(C=C)_{aromatic}$, 1232 $\nu(C-O)_{phenolic}$, 519 ν(Cu–O), 444 ν(Cu–N). UV–vis (DMF, λ_{max}, 1.0×10^{-3} M): 507, 440, 413, 325, 276.

$[CuA^3(Cl)(H_2O)]$: $C_{16}H_{18}ClCuNO_5$. Yield: 73%, color: Dark green, melting point: >250 °C. Elemental analysis; found (calcd.) %; C, 47.69 (47.65); H, 4.56 (4.50); N, 3.55 (3.47). Mass spectrum (ESI/MS, *m*/*z*): Calcd.: 373.29, found: 373 $[M]^+$; calcd.: 319.82, found: 320.44 $[M-H_2O-Cl]^+$. FTIR (KBr, ν, cm^{-1}): 3320 $\nu(O-H)_{H2O}$, 2942 $\nu(C-H)_{aliph}$, 1598 ν(C=N), 1482 $\nu(C=C)_{aromatic}$, 1287 $\nu(C-O)_{phenolic}$, 535 ν(Cu–O), 447 ν(Cu–N). UV–vis (DMF, λ_{max}, 1.0×10^{-3} M): 503, 441, 415, 379, 276.

2.4. X-ray crystallography

Bruker D8 QUEST diffractometer using Mo-*Kα* radiation ($\lambda = 0.71073$ Å) was used to collect X-ray crystallographic data for bidentate ligands (HA^2 and HA^3) [13]. The reflection data were collected at 273 K. The structures of the compounds were solved by the direct method SHELXS97 and refined against F^2 using full-matrix least-squares refinement using SHELX2014/6 [14,15]. All atoms except hydrogens were refined using anisotropic atomic displacement parameters. Hydrogen atoms bonded to carbon and oxygen atoms were located at calculated positions using a riding model and refined with temperature factors riding on the carrying atoms. The crystallographic data for bidentate ligands (HA^2 and HA^3) are presented in Table 1. Bond lengths and angles are given in the supplementary documents (Table S1&S2).

Table 1
Crystallographic data for the complexes.

Identification code		HA2	HA3
Empirical formula		$C_{16}H_{17}NO_4$	$C_{16}H_{17}NO_4$
Formula weight		287.30	287.30
Crystal system		*Monoclinic*	*Tetragonal*
Space group		*I2*	$P4_12_12$
Unit cell	a (Å)	10.7746(6)	6.7446(2)
	b (Å)	25.4384(15)	6.7446(2)
	c (Å)	11.3786(6)	64.410(3)
	α (°)	90	90
	β (°)	104.928(4)	90
	γ (°)	90	90
Volume (Å^3)		96.500(6)	2930.0(2)
Z		8	8
Calculated density (mg/cm^3)		1.232	1.303
Abs. coeff. (mm^{-1})		0.089	0.094
Refl. collected		8979	4489
Ind. Refl. [R_{int}]		6054 [0.0289]	2861 [0.0662]
Comp. to $\Theta = 25.242°$		99.6%	97.9%
R1, w*R*2 [I > 2σ (I)]		0.0601, 0.0858	0.1290, 0.3009
R1, w*R*2 (all data)		0.1272, 0.1147	0.1518, 0.3166
Goodness-of-fit on F^2		0.965	1.095
CCDC number		1919490	1919491

2.5. Preparation of microbial culture

The Schiff base ligands and their Cu^{2+} metal complexes were evaluated *in vitro* antibacterial and antifungal activity against the *Staphylococcus aureus* Rosenbach ATCC-6538, *Bacillus subtilis* Ehrenberg ATCC-14028 and *Bacillus cereus* ATCC 7064 (as Gram-positive bacteria), *Escherichia coli* ATCC-8739, *Salmonella typhimurium* (as Gram-negative bacteria) and *Candida albicans* ATCC-90028 (fungi) by agar-well diffusion. In the antimicrobial activity studies, Müller Hilton Agar (MHA) for bacteria was used as a stock medium and Malt Extract Agar (MEA) for the yeast strain. The antimicrobial activity studies were carried out according to a known method [16].

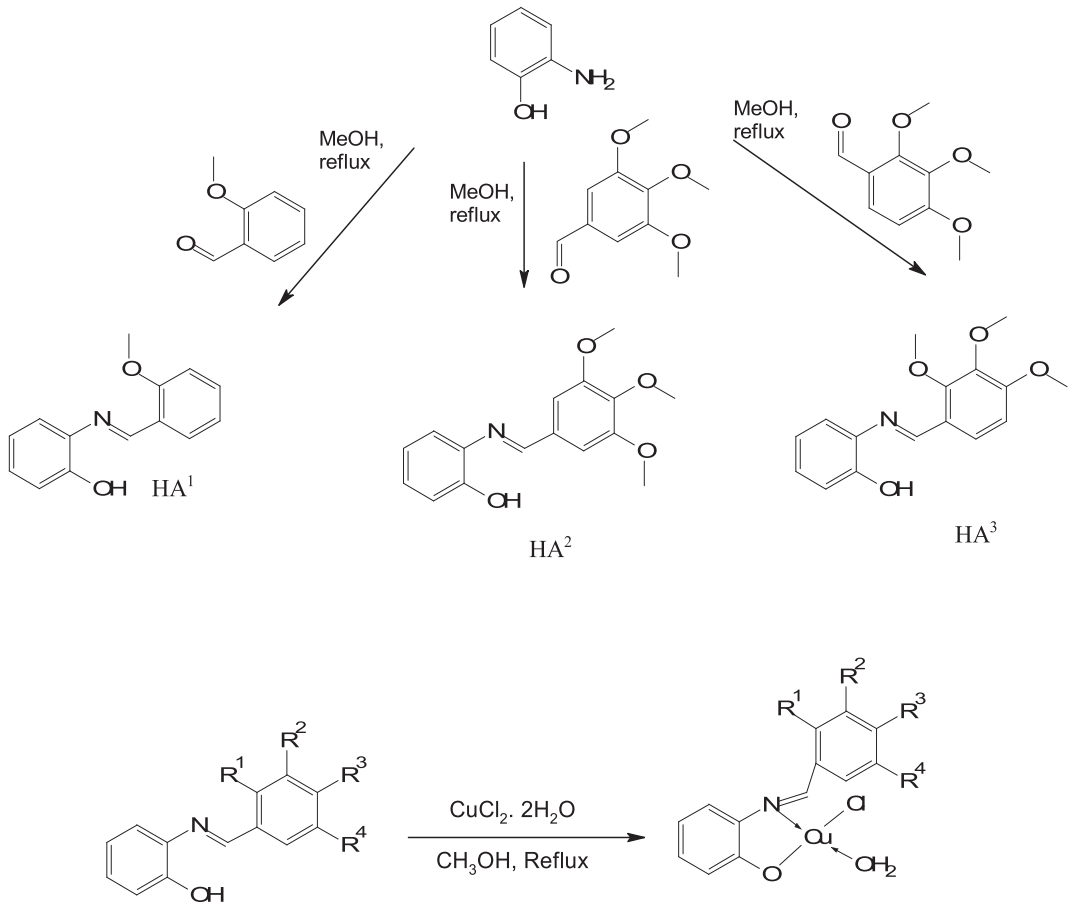

Fig. 1. Synthesis route of the bidentate Schiff base ligands and their Cu(II) transition metal complexes.

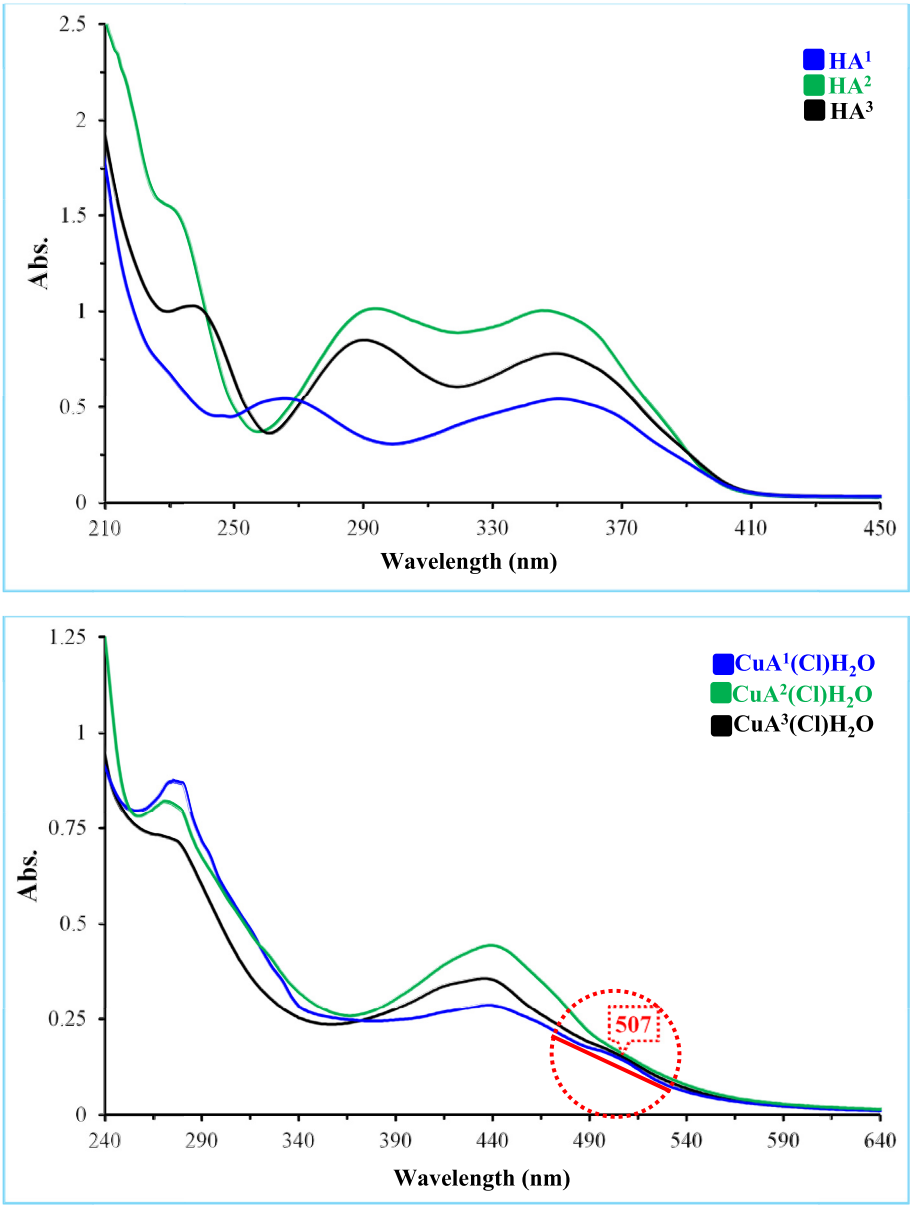

Fig. 2. The UV–vis spectra of the ligands and their Cu^{2+} metal complexes in the 1.0×10^{-3} M DMF solution.

Compounds (20 μL) in DMSO/H_2O (1:9) were pipetted into the hollow agar at concentration 12.5 mg/mL. The petri dishes were left at 4 °C for 2 h and then the plates were incubated at 37 ± 1 °C for bacterium and 25 ± 1 °C fungi (18–24 h). At the end of this period, inhibition zones formed on the medium were determined as millimeters (mm). The disc containing DMSO, Amikacin (AK: 30 μg) and Gentamicin (CN: 10 μg) were used for control.

Minimal inhibitory concentrations (MIC) of the ligands and their Cu(II) complexes were obtained by using the serial dilution technique [16]. Prior to this study, compounds were dissolved in DMSO/H_2O (1:9) to make a 12.5 mg/mL stock and then diluted to 1.25 and 0.125 mg/mL. The results were expressed in milligrams per milliliter. The minimum inhibition concentration (MIC) values for the ligands (HA^1-HA^3) and their Cu^{2+} metal complexes are given in the supplementary file.

3. Results and discussion

In this study, we prepared three aromatic imine ligands (HA^1-HA^3) from the reaction of the *o*-aminophenol and methoxy benzaldehyde derivatives (Fig. 1). The ligands have been characterized by using the analytical and spectroscopic methods. Since the ligands have a polar character, they are readily soluble in polar organic solvents. In addition, they can be stored at the 25 °C for a long time without degradation. The Cu^{2+} complexes of the ligands were prepared in 1:1 M ratio. In addition, the ligands and their Cu^{2+} complexes were found to be non-hygroscopic. This situation was confirmed by analytical and spectroscopic data. It was also confirmed by the results of thermal analysis that the ligands do not have hygroscopic property. Since all ligands have the bidentate character, when they interact with copper ions in the methanol solution, they form complexes in the 1: 1 M ratio.

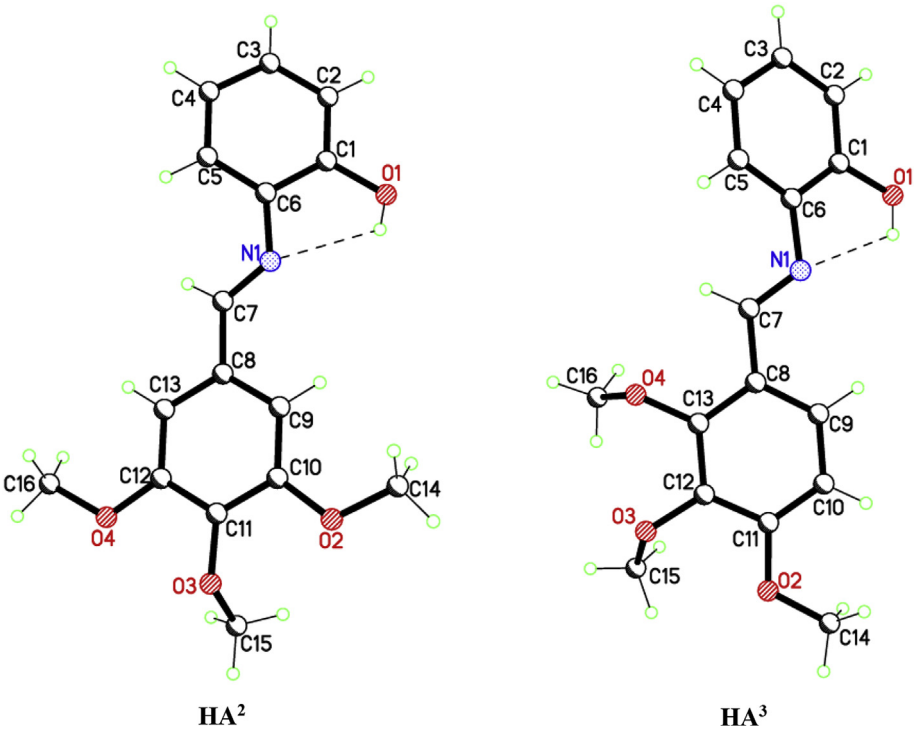

Fig. 3. Molecular structures of HA^2 and HA^3 with atom numbering.

3.1. Spectroscopic characterization of the bidentate ligands and their Cu^{2+} complexes

So as to characterize the 2-aminophenol based imine ligands and their Cu^{2+} complexes, their FTIR spectral properties were investigated and obtained spectral properties were given in the experimental section. The FTIR spectra of the HA^3 and its $[CuA^3(Cl)(H_2O)]$ complex are given in the supplementary file (Fig. S1). In the spectra of the ligands, the stretching vibrations in the 3376-3350 cm^{-1} range refer to the ν(O—H) group. After complexation, this band became a wide band and observed in the range of 3342—3320 cm^{-1}. Because, in the structure of the complexes, there is H_2O molecule that coordinated to the metal ion. The azomethine group (CH═N) of the imine ligands were observed in the 1624-1616 cm^{-1} range. Since the nitrogen atom of the azomethine group has a donor property, during the complexation, as the nitrogen atom coordinates to the Cu^{2+} ion, the azomethine group stretchings shifted to the lower wavenumbers (1600-1596 cm^{-1}). In the spectra of the complexes, the bands in the 542—519 and 478-444 cm^{-1} range can be attributed to the ν(Cu—O) and ν(Cu—N), respectively.

The electronic spectral properties of the bidentate ligands and their Cu^{2+} complexes were studied DMF (1.0×10^{-3} M) and the spectral results are given in the experimental section. The UV—vis

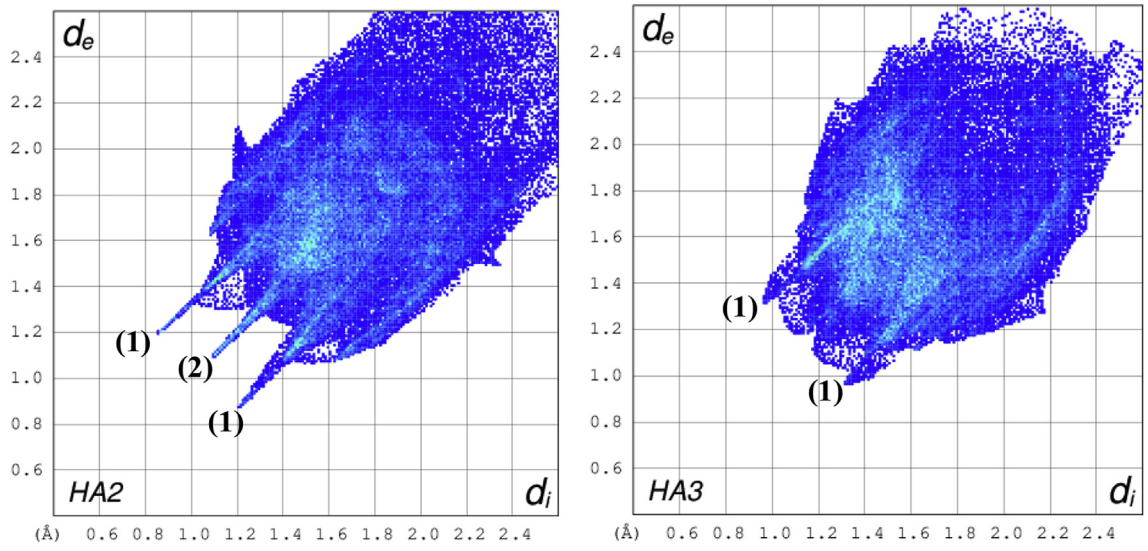

Fig. 4. Fingerprint plots of HA^2 and HA^3. Spikes indexed as (1) and (2) show H···O/O···H and H···H, respectively.

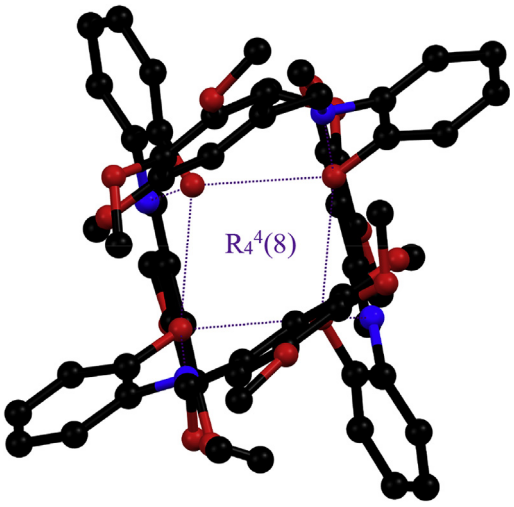

Fig. 5. Hydrogen bonded tetramer in the structure of HA^2. Hydrogen bonds are shown as dashed lines.

spectra of all compounds are presented in Fig. 2. In the UV–vis spectra of the ligands, the absorption bands in the 389-343 nm range come from the n-π* transitions. The π-π* and π-δ* transitions are shown in the 290-230 nm range. As different from the electronic properties of the ligands, the Cu^{2+} complexes show the d-d transitions in the 507-503 nm range. The absorption bands at 440 nm may be assigned to the charge transfer band (M→ L or L→M). Upon complexation with Cu^{2+}, the n-π* transitions shifted to the lower wavelength (379-325 nm range). On the other hand, the π-π* and π-δ* transitions in the spectra of the complexes were seen at the 276 and 271 nm, respectively.

The mass spectra of the complexes were obtained and the data are given in the experimental section. The ESI mass spectra of the ligands were given in the Supplementary documents (Fig. S2). In the mass spectra of all compounds, the molecular ion peaks $[M]^+$ were observed. All compounds suffer from mass loss on a regular basis and they have similar fragmentation ions.

The ^1H–^{13}C NMR spectra of the ligands were recorded in $CDCl_3$ and TMS as internal standard and obtained spectral data were given in the experimental section. While the 3,4,5-trimethoxy benzaldehyde, which is one of the carbonyl compounds used to synthesize the ligands, has a symmetrical, the hydrogen atoms of the other carbonyl compounds (2-methoxy and 2,3,4-trimethoxy benzaldehyde) are asymmetric nature. That is, these structural features are retained in the resulting ligands. In the ^1H NMR spectra of the ligands, the signal for the phenolic hydroxy proton of the ligands appears to be a weak and broad singlet around 9.5 ppm. The signals in the 8.66–8.56 ppm range may be arised from the hydrogen atom of the azomethine group (CH═N). In the structure of the ligands, there are two aromatic rings. These are phenol and phenyl rings. The multiplets belonging to the aromatic rings hydrogen atoms are shown in the 8.02–6.28 ppm range. The hydrogen atoms of the $-OCH_3$ group of the ligand HA^1 are shown at 3.90 ppm as a singlet. In the ligand HA^2, the hydrogen atoms of the methoxy groups were observed at 3.75 and 3.82 ppm because they had an equivalent environment. But, the ligand HA^3, the hydrogen atoms of the methoxy groups are in the 3.98–3.85 ppm range.

The ^{13}C NMR spectra for the ligands have also been investigated. The signals belonging to the carbon atom of the azomethine group in the ligands were seen in the 167.80–164.55 ppm range. The aromatic ring carbon atoms of the ligands were observed in the range of 159.72–108.40 ppm. The methoxy group carbon atoms in the ligands were seen in 61.50–56.45 ppm range.

3.2. Molecular structures of HA^2 and HA^3

Molecular structures of the HA^2 and HA^3 were further characterized by X-ray diffraction studies. The structures of HA^2 and HA^3 were depicted in Fig. 3. The asymmetric unit of HA^2 contains two crystallographically independent ligand molecules with similar bond lengths and angles. Molecular structures of the ligands are broadly similar differing in the position of methoxy groups and hydrogen bond interactions within the structures. In the structure of both ligands, the imine bond distances are within the range of the carbon nitrogen double bond (C═N) distances. The independent molecules in the asymmetric unit of HA^2 differ from the dihedral angles between the phenyl and phenol rings. The phenyl (C1/C6) and phenol rings (C8/C13) are tilted at 21.424(15)° for HA^2 and 21.424(15)° for HA^3. This may be due to the different intermolecular interactions within structures.

Although the structures of HA^2 and HA^3 are similar, packing of molecules are widely different due to the different hydrogen bond interactions within each structure. In order to investigate the intermolecular contacts between neighbouring molecules, Hirshfeld surfaces for both ligands were drawn. The 2D fingerprint plots of ligands HA^2 and HA^3 are not similar due to different intermolecular contacts between the ligand molecules (Fig. 4). Both compounds show an expected phenol-imine hydrogen bond (OH·····N) forming a S(5) hydrogen bond motif. In the structure of HA^2, the phenolic group (O1) also involves in intermolecular

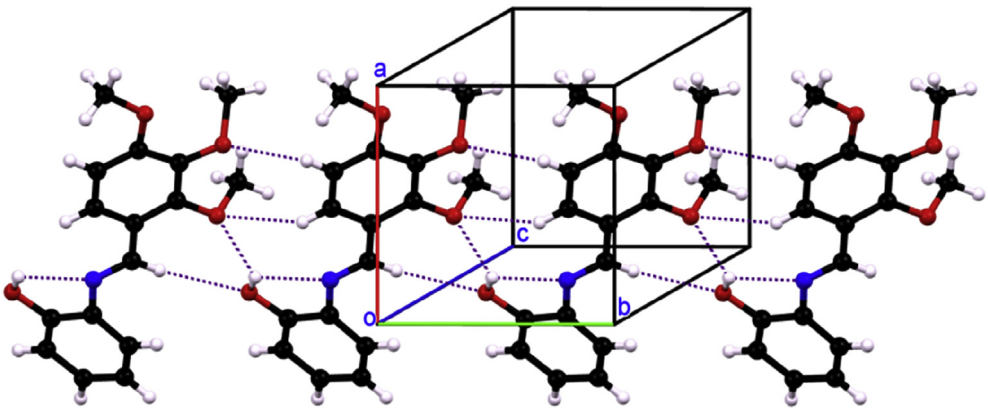

Fig. 6. Packing diagram of HA^3 showing CH···O contacts.

hydrogen bonding with the phenolic oxygen atom (OH$\cdots$O) of an adjacent molecule. The HA^2 molecules form a tetramer connected by O–H$\cdots$O hydrogen bonds between phenolic groups producing a $R_4^4(8)$ motif (Fig. 5). Hydrogen bond parameters for HA^2 and HA^3 are given in the supplementary documents (Table S3&S4). In the 2D fingerprint plot of HA^2 (Fig. 4), the hydrogen bond contacts (OH$\cdots$O) are seen as two sharp spikes (1). The spiked indexed as (2) is due to the H$\cdots$H contacts. Moreover, these hydrogen bond contacts between the phenolic groups are observed in the d_n surface as intense red spots (Fig. S3). HA^2 molecules are further linked by CH$\cdots$O contacts. In the structure of HA^3, there is no intermolecular hydrogen bond contacts between the phenolic group of adjacent molecules. Molecules are linked by $CH_{phenyl}\cdots O$ interactions as shown in Fig. 6. The relatively close H$\cdots$O interactions are seen as red spots in the *dn* surface and two broad spikes in the 2D finger print plot (Fig. 4). In structure of both compounds, phenyl-phenyl stacking interactions were not observed.

3.3. The electrochemical of the ligands and their metal complexes

The redox properties of the organic ligands and their Cu^{2+} metal complexes have been identified in the 1.0×10^{-3} M DMF solution and obtained electrochemical data are given in Table 2. The redox properties of the compounds were studied in the $-2.0 - (+2.0)$ V range and 100–1000 mV/s scan rate. The glassy carbon electrode was used as the working electrode during the electrochemical study, on the other hand, Ag^+/AgCl was used as the reference electrode and Pt was used as the counter electrode. The cyclic voltammograms of the ligands HA^1-HA^3 have given in Fig. 7. To understand the redox properties of the ligands and Cu(II) complexes, the electrochemical properties of the starting compounds (Fig. S4), the methoxy aldehyde derivatives, were examined under the same experimental conditions. All of aldehyde compounds showed similar redox behavior. In the −2.0 - (+) 2.0 V range cathodic and anodic scaning area, the starting compounds have two anodic and two cathodic peak potentials. The cathodic and anodic redox couples have similar values in positive and negative regions. The cathodic values in the negative region are in the −0.47-(-0.34) V range. In addition, positive cathodic values are in the range of 0.53–0.33 V. On the other hand, in the anodic region, while the negative anodic values are in the −0.12-(-0.34) V range, the positive values are in the 0.05–0.26 V range. While the cathodic peak potentials shift to the more positive region due to increased scanning speed, the anodic peak potentials shifted to the negative regions. All redox processes of the starting materials are irreversible.

The ligand HA^1 has two cathodic and two anodic peak potentials in the −0.54-0.15 and −0.38-0.28 V range, respectively. The redox processes are irreversible at all scan rates and the electrochemical values have shifted to the more negative regions than the 2-methoxy benzaldehyde (starting material). However, the ligands HA^2 and HA^3 have three cathodic peaks in the −0.55-(+0.84) V range and there are two anodic peaks in the −0.42-(+0.19) V range and all redox couples are irreversible. In the cyclic voltammetry sudies of the Cu^{2+} complexes, in the forward scan (cathodic scan), cathodic values for the $[CuA^1(Cl)(H_2O)]$ and $[CuA^2(Cl)(H_2O)]$ show one cathodic and two anodic peaks in the 0.75–0.62 and −0.41-0.27 V range, respectively. The complex $[CuA^3(Cl)(H_2O)]$ has three anodic and two cathodic peaks in the −0.55-0.84 and −0.34-0.22 V range, respectively. In the $[CuA^3(Cl)(H_2O)]$, the cathodic and anodic values shifted to the more positive regions owing to the positions of the methoxy groups on the phenyl ring. The obtained results offer a strong interaction between Cu(II) and ligands. In the complexes, redox processes are the metal centred. In the consecutive redox couple of Cu(II)/Cu(0), the cathodic peak results from the reduction of Cu(II) to Cu(0) and the anodic peak is for the oxidation of Cu(0) to

Table 2
Electrochemical data of the ligands HA^1-HA^3 and their Cu^{2+} complexes in the 1.0×10^{-3} M DMF solution.

Compound	Scanrate (mV/s)	E_{pc}(V)	E_{pa}(V)	E_{pa}/E_{pc}	$E_{1/2}$(V)	ΔE_p(V)
HA^1	100	0.05	0.28, −0.07	5.60	–	0.23
	250	−0.45, 0.10	0.17, −0.21	1.70	–	0.07
	500	−0.49, 0.12	0.09, −0.30	0.75	–	−0.03
	750	−0.51, 0.14	0.04, −0.35	0.68	–	−0.10
	1000	−0.54, 0.15,	0.01, −0.38	0.70	–	−0.14
	100	0.62	0.27, −0.17	0.43	–	−0.35
$[CuA^1(Cl)(H_2O)]$	250	0.64	0.23, −0.23	0.35	–	0.41
	500	0.68	0.16, −0.28	0.23	–	−0.52
	750	0.70	0.13, −0.32	0.18	–	−0.57
	1000	0.74	0.10, −0.33	0.13	–	−0.64
	100	−0.55, 0.10, 0.75	0.16, −0.23	1.60	–	0.06
HA^2	250	−0.50, 0.16, 0.73	0.09, −0.30	0.60	–	−0.07
	500	−0.47, 0.19, 0.69	0.10, −0.35	0.52	–	−0.09
	750	−0.45, 0.23, 0.62	0.11, −0.39	0.47	–	−0.03
	1000	−0.47, 0.25, 0.58	0.07, −0.42	0.89	–	0.05
	100	0.64	0.27, −0.19	0.42	–	−0.37
$[CuA^2(Cl)(H_2O)]$	250	0.67	0.21, −0.28	0.31	–	−0.46
	500	0.71	0.16, −0.33	0.22	–	−0.55
	750	0.73	0.12, −0.36	0.12	–	−0.61
	1000	0.75	0.07, −0.41	0.09	–	−0.68
	100	−0.51, 0.07, 0.52	0.19, −0.20	0.39	–	0.12
HA^3	250	−0.49, 0.09, 0.57	0.14, −0.25	0.51	–	0.05
	500	−0.46, 0.13, 0.61	0.10, −0.27	0.58	–	−0.03
	750	−0.45, 0.14, 0.63	0.08, −0.31	0.57	–	−0.06
	1000	−0.46, 0.16, 0.65	0.04, −0.33	0.71	–	0.13
	100	−0.55, 0.31, 0.81	0.22, −0.32	0.70	–	−0.09
$[CuA^3(Cl)(H_2O)]$	250	−0.53, 0.32, 0.82	0.17, −0.30	0.57	–	−0.14
	500	−0.49, 0.33, 0.84	0.14, −0.31	0.69	–	0.18
	750	−0.53, 0.34, 0.75	0.10, −0.34	0.64	–	0.19
	1000	−0.55, 0.35, 0.77	0.10, −0.32	0.58	–	0.23

All the potentials are referenced to Ag+/AgCl; where Epa and Epc are anodic and cathodic potentials, respectively. ΔEp = Epa−Epc. E1/2 = 0.5 x (Epa + Epc). Concentration: 1.0 x 10-3 M DMF.

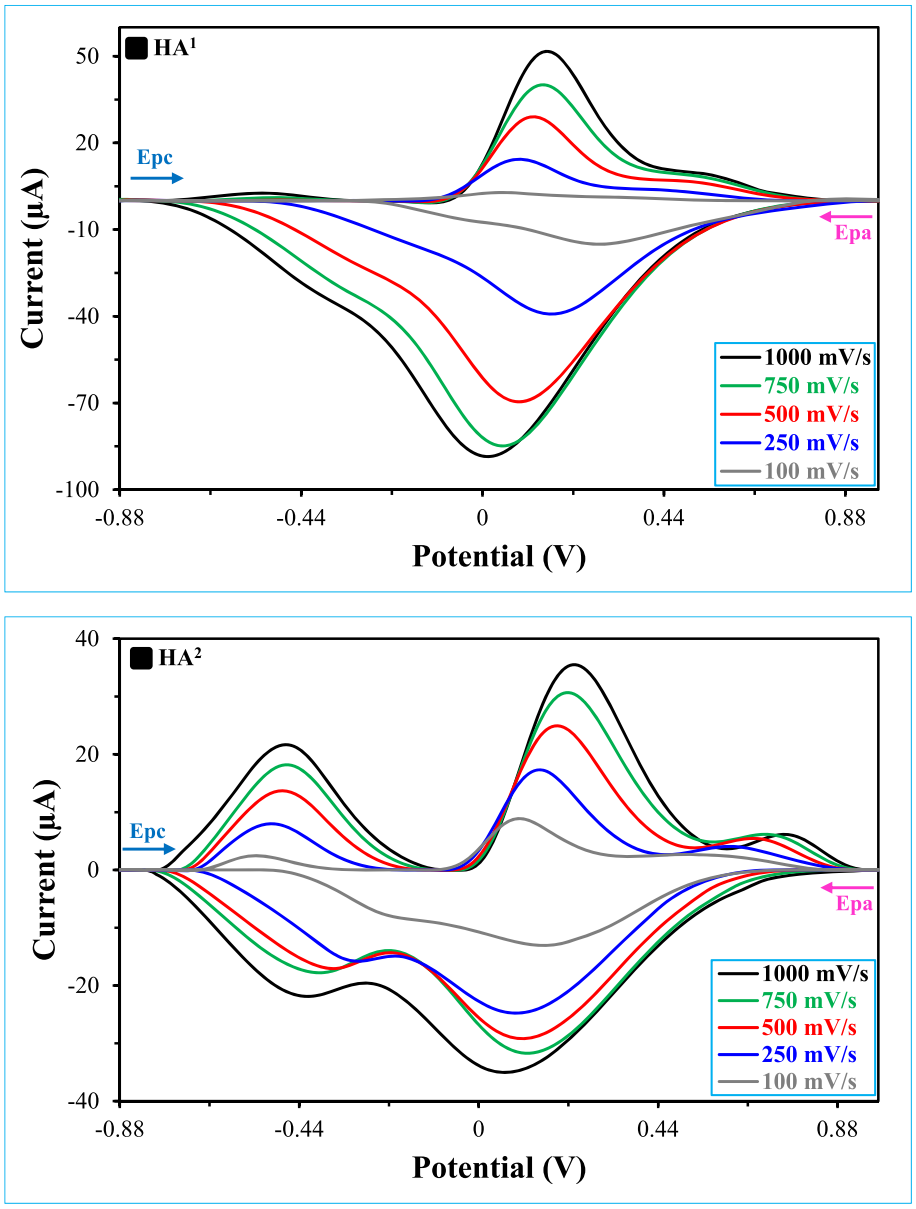

Fig. 7. The cyclic voltammograms of the ligands in the 1.0×10^{-3} M DMF solution and 100-1000 mVs^{-1} scan rates.

Cu(II).

3.4. The thermal properties of the ligands and their metal complexes

Thermal properties of the compounds were investigated in the 20–800 °C temperature range. Thermal decomposition curves of the ligands HA^1-HA^3 and their $[CuA^n(Cl)H_2O]$ (n: 1, 2, 3) complexes in the 20–900 °C temperature range are shown in Fig. 8. Thermal degradation curves show that the ligands and their metal complexes do not contain adsorbed water molecules. The TGA curves of the ligands and their metal complexes show the similar decomposition processes. The ligands are stable up to 210 °C. The ligands decompose at two steps. The process of degradation of the ligands begins at about 213 °C. At first step, a large proportion of the masses of ligands have lost. As can be seen also from the thermal degradation curves, the ligand HA^1 is more unstable than the other ligands. Thermal stability of the ligand HA^2 is higher than the other ligands. At the second step, the remaining part of the decomposition of the ligands is completely degraded to CO_2, H_2O and N_xO_y gases. In the DTA curves of the ligands, the degradation of the ligands corresponds to the strong endothermic peaks. In the TGA curves of the Cu^{2+} complexes, thermal decomposition process takes place in four steps. At the first step, the coordinated water molecules to the Cu^{2+} ions move away from the complexes in the 110–130 °C temperature range. At the second step, the coordinated Cl^- ion to the metal ions is lost at about 218 °C temperature. At the third and fourth steps, the organic parts of the remaining residues start the decomposition at about 350 °C and the decomposition process continues up to the 800 °C temperature. The final product obtained by degradation of the complexes is metal oxide (CuO).

3.5. The biological activity properties of the ligands and their metal complexes

Fungicidal and bactericidal activities of the bidentate Schiff base

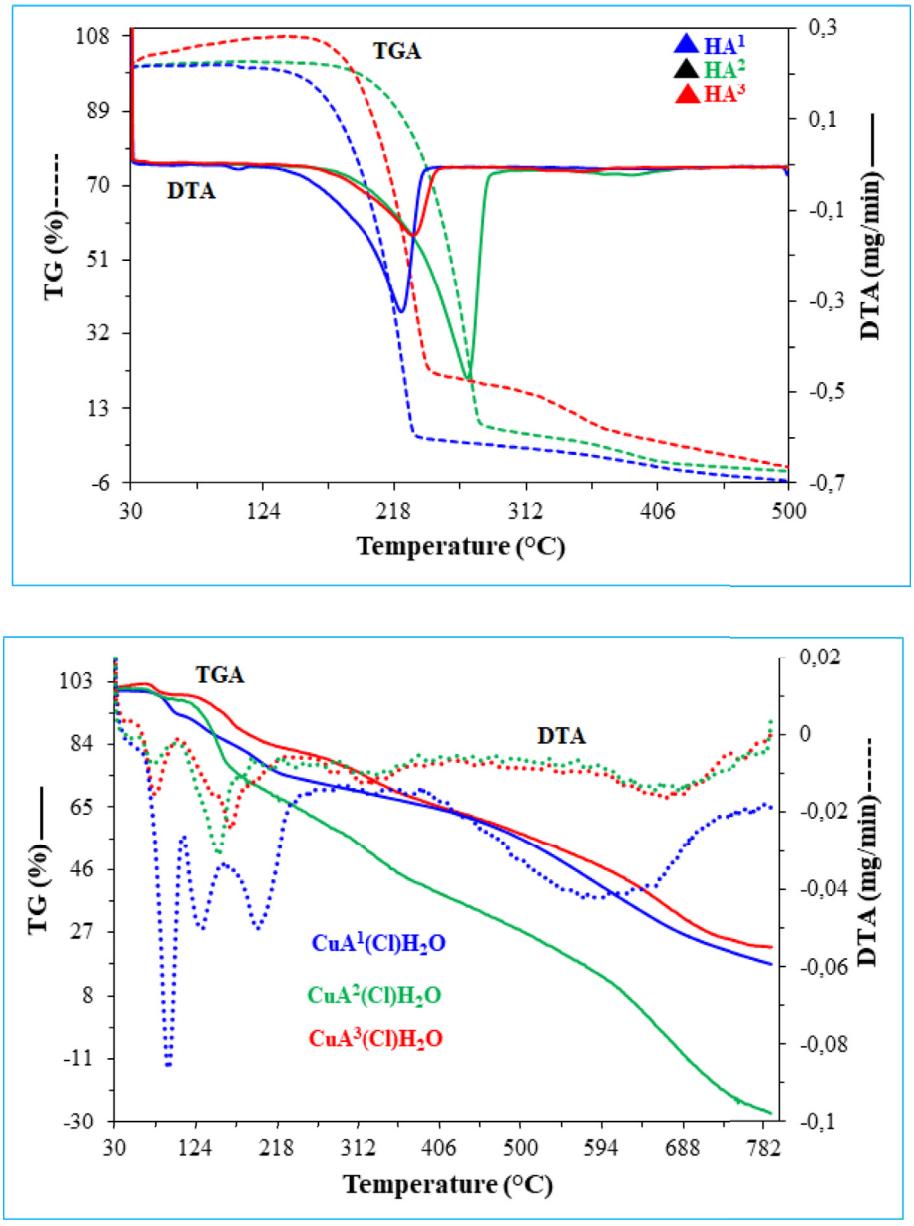

Fig. 8. Thermal curves of the ligands and their Cu^{2+} complexes in the 20–800 °C temperature range.

ligands (HA^1-HA^3) and their Cu^{2+} complexes against photogenic bacteria and fungi were given in Table 3. Comparison of the antimicrobial activity properties of the bidentate ligands and their Cu^{2+} transition metal complexes is shown in Fig. S5. In the antimicrobial activity studies, we used the *Staphylococcus aureus*, *Bacillus subtilis* and *Bacillus cereus* as the gram positive; *Escherichia coli* and *Salmonella typhimurium* as the gram negative and *Candida albicans* as the fungi. Gentamicin and amikacin antibiotics were used as positive control groups. The sensitivity of a microorganism to antibiotics and other antimicrobial agents was determined by the assay plates which were incubated at 25 °C for three days for yeasts and at 37 °C for 18–24 h for bacteria. Some of the tested compounds showed a remarkable biological activity against different types of Gram-positive and Gram-negative bacteria. The ligands containing the nitrogen (N) and oxygen (O) donor atoms have the power to inhibit enzyme production. Because enzymes need free hydroxy groups for their activity seem to the particularly susceptible to deactivation by the metal ions existed in the complexes. The diversity in the impressiveness of various biocidal drugs against different organisms [17] has attached to the impermeability of the cell. The organic compounds behave as a lipophilic group [18] to take out the compound through the semipermeable membrane of the cell. The synthesized ligands have the ability to form chelates between the azomethine nitrogen atom and the phenolic hydroxyl groups. In the ligands, there are π-electron delocalization throughtout the molecules. The donor groups (such as methoxy groups) on the benzene rings give the electron to the rings. Therefore, the chelate forming in the molecule diminishes the polarity of the central ion. This chelation enhances the lipophilic structure of the central atom that allows the membrane to pass through the lipid layer.

It has been determined that the complexes have different antimicrobial activity on microorganism strains. While the gram-positive, gram-negative and yeast strains generally had a

Table 3
Antimicrobial activity values of the bacteria and fungi (mm).

	Gram (-) bacteria		Gram (+) bacteria		Fungi
Compounds	*E. coli*	*S. typhimurium*	*S. aureus*	*B.cereus*	*C. albicans*
HA^{1}*	–	8	12	–	8
$[CuA^{1}(Cl)(H_2O)]$	12	12	14	12	–
HA^{2}	–	–	–	–	–
$[CuA^{2}(Cl)(H_2O)]$	10	18	20	16	8
HA^{3}	–	–	–	–	–
$[CuA^{3}(Cl)(H_2O)]$	12	16	18	18	8
Amikacin	16	18	18	22	–
Gentamicin	12	18	18	16	–
DMSO	–	–	–	–	–

-: Zone was not shown. * Compounds (20 μL) in DMSO/H2O (1:9) were pipetted into the hollow agar at concentration 12.5 mg/mL.

minimum inhibition concentration of 12.5 mg/mL, whereas in some strains this ratio was found to be 1.25 mg/mL. It is thought that these different findings may be caused by the presence of specific cell wall structure of each strain. The ligands HA^{2} and HA^{3} do not activity against to the any microorganisms (see Table 3). On the other hand, the Cu^{2+} complexes of these ligands show the same effect towards the bacteria and yeast. Because the structures of ligands and metal complexes are similar, such a situation may have been observed.

4. Conclusion

The spectral and analytical data revealed that the general formula of the Cu^{2+} metal complexes coordinated to bidentate imine ligands (HA^{1}-HA^{3}) is $[Cu(A)^{n}(Cl)(H_2O)]$(where $n = 1–3$). The spectroscopic data proposed that the mononegative bidentate imine ligands natured as O, N-donor sequence towards coordination with the Cu^{2+} metal ions. The presence of one coordinated aqua ligands in the Cu^{2+} metal complexes was confirmed by thermal study such as TGA and DTA. Similarly, the existence of one coordinated chlorine atom in the Cu^{2+} metal complexes was also confirmed by thermal study. The single crystals of the ligands HA^{2} and HA^{3} have been obtained from the MeOH solution and their molecular structures were solved by the X-ray technique. Antimicrobial activity studies of the bidentate ligands and their Cu^{2+} metal complexes were studied using the *S. aureus, E. coli, B. cereus, B. subtilis, S. typhimurium* as bacteria and *C. albicans* as fungi and the complex Cu^{2+} of the ligand HA^{2} showed the highest activity against to the *S. aureus*. While the ligands HA^{2} and HA^{3} do not show the activity versus to the bacteria and fungi, the ligand HA^{1} has the activity against to the *S. typhimurium, S. aureus* and *C. albicans*.

Appendix A. Supplementary data

Supplementary data to this article can be found online at https://doi.org/10.1016/j.molstruc.2019.127059.

References

[1] M. Tümer, H. Köksal, M. Kasım Şener, S. Serin, Trans. Met. Chem. 24 (1999) 414.
[2] M. Tümer, C. Çelik, H. Köksal, S. Serin, Trans. Met. Chem. 24 (1999) 525.
[3] A. Hameed, M. al-Rashida, M. Uroos, S.A. Ali, K.M. Khan, Expert Opin. Ther. Pat. 27 (2017) 63.
[4] W. Radecka-Paryzek, I. Pospieszna-Markiewicz, M. Kubicki, Inorg. Chim. Acta 360 (2007) 488.
[5] J.H. Jia, X.M. Tao, Y.J. Li, W.J. Sheng, Chem. Phys. Lett. 514 (2011) 114.
[6] K. Tanaka, R. Shimoura, M.R. Caira, Tetrahedron Lett. 51 (2010) 449.
[7] G. Ceyhan, M. Köse, V. McKee, S. Uruş, A. Gölcü, M. Tümer, Spectrochim. Acta, Part A 95 (2012) 382.
[8] M. Jaworska, M. Wełniak, J. Zięciak, A. Kozakiewicz, A. Wojtczak, Arkivoc ix (2011) 189.
[9] P.G. Gozzi, Chem. Soc. Rev. 33 (2004) 410.
[10] A. Fernandez, D. Vazquez-Garcıa, J.J. Fernandez, M. Lopez-Torres, A. Suarez, S. Castro-Juiz, J.M. Vila, New J. Chem. 26 (2002) 398.
[11] H.C. Polonini, L.L. Lima, K.M. Gonçalves, A.M.R. do Carmo, A.D. da Silva, N.R.B. Raposo, Bioorg. Med. Chem. 21 (2013) 964.
[12] E. Tauer, K.H. Grellmann, J. Org. Chem. 46 (1981) 4252.
[13] Bruker, APEX2 and SAINT Bruker, AXS Inc, 1998.
[14] G.M. Sheldrick, Acta Crystallogr. A. 64 (2008) 112.
[15] G.M. Sheldrick, Acta Crystallogr. C 71 (2015) 3.
[16] a) M. Balouiri, M. Sadiki, S.K. Ibnsouda, J. Pharm. Anal. 6 (2016) 71;
b) Clinical and Laboratory Standards Institute (CLSI), Reference Method for Broth Dilution Antifungal Susceptibility Testing of Filamentous Fungi; Approved Standard Second - Edition CLSI Document M38-A2, 940, West valley Road, Suite 1400, Clinical and Laboratory Standards Institute, Wayne, Pennsylvania, 2008, ISBN 1-56238-668-9, 19087-1898 (USA);
c) National Committee for Clinical Laboratory Standards (NCCLS), Document M31-A Performance Standards for Antimicrobial Disk and Dilution Susceptibility Tests for Bacteria Isolated from Animals, 1999, p. 57 (Villanova: approved standard NCCLS);
d) NCCLS National Committee for Clinical Laboratory Standards, Reference Method for Broth Dilution Antifungal Susceptibility Testing of Yeasts: Proposed Standard, NCCLS, Villanova, 2002.
[17] P.G. Lawrence, P.L. Harold, O.G. Francis, Antibiot. Chemother. 5 (1980) 1597.
[18] S. Rich, J.G. Horsfall, Phytopathology 42 (1952) 457.